THE MECHANICAL DESIGN OF SPIDER SILKS: FROM FIBROIN SEQUENCE TO MECHANICAL FUNCTION

J. M. GOSLINE*, P. A. GUERETTE, C. S. ORTLEPP AND K. N. SAVAGE

Department of Zoology, University of British Columbia, Vancouver, British Columbia, Canada V6T 1Z4

*e-mail: gosline@zoology.ubc.ca

Summary

Spiders produce a variety of silks, and the cloning of genes for silk fibroins reveals a clear link between protein sequence and structure–property relationships. The fibroins produced in the spider's major ampullate (MA) gland, which forms the dragline and web frame, contain multiple repeats of motifs that include an 8–10 residue long poly-alanine block and a 24–35 residue long glycine-rich block. When fibroins are spun into fibres, the poly-alanine blocks form β-sheet crystals that crosslink the fibroins into a polymer network with great stiffness, strength and toughness. As illustrated by a comparison of MA silks from *Araneus diadematus* and *Nephila clavipes*, variation in fibroin sequence and properties between spider species provides the opportunity to investigate the design of these remarkable biomaterials.

Key words: spider, *Araneus diadematus*, *Nephila clavipes*, silk, fibroin, structure/property relationship.

Introduction

Orb-web-spinning spiders produce a variety of high-performance structural fibres with mechanical properties unmatched in the natural world and comparable with the very best synthetic fibres produced by modern technology. As a result, there is considerable interest in the design of these materials as a guide to the commercial production of protein-based structural polymers through genetic engineering. To understand the design of silks, we must understand the relationships between structure and function, and this will require information from molecular biology, polymer physics, materials science and spider biology. We now have good information on the amino acid sequence motifs present in spider fibroins, and our understanding of the molecular architecture of spider silks is growing daily. Unfortunately, in many cases, our understanding of silk design is flawed because we do not know which mechanical properties are crucial to its function. To quote Wainwright (1988), 'Identification of the properties that are important to a particular function requires all the intuitive insights and creative abilities of objective scientists.' Only when we understand the true function of spider silks will be able determine whether a spider's dragline silk offers an appropriate model for man-made materials produced through genetic engineering.

The function of spider silks

The orb-web-weaving araneid spiders provide ideal model organisms for studying the functional design of protein-based structural materials. These spiders have seven different gland–spinneret complexes, each of which synthesizes a unique blend of structural polymers and produces a fibre with a unique set of functional properties (Gosline et al., 1986; Vollrath, 1992). Unfortunately, our knowledge of functional relationships for most of these materials is very limited, with the exception of the major ampullate (MA) gland fibres and to some extent the viscid silk fibres produced by the flagelliform (FL) gland. The organization of these fibres in the spider's orb-web is illustrated in Fig. 1, where it can be seen that MA silk fibres form the web frame and the spider's dragline. The viscid silk forms the glue-covered catching spiral.

Mechanical properties of MA and viscid silks

Fig. 1 shows typical tensile test data for MA and viscid silk from the spider *Araneus diadematus* plotted as stress–strain curves. The stress (σ) is the normalized force (F), defined as $\sigma = F/A$, where A is the initial cross-sectional area of the silk fibre. The strain (ε) is the normalized deformation, defined as, $\varepsilon = \Delta L/L_0$, where L_0 is the fibre's initial length, and ΔL is the change in fibre length. The slope of the stress–strain curve gives the stiffness of the material, and the maximum values of stress and strain at the point where the material fails give the strength (σ_{max}) and extensibility (ε_{max}), respectively. The area under the stress–strain curve gives the energy required to break the material, and this variable can be used to quantify toughness. Values for the stiffness, strength, extensibility and toughness of these two spider silks, along with values for other biomaterials and selected man-made materials, are presented in Table 1.

Note that MA silk is stiffer than the other polymeric biomaterials listed, although mineralized biomaterials may
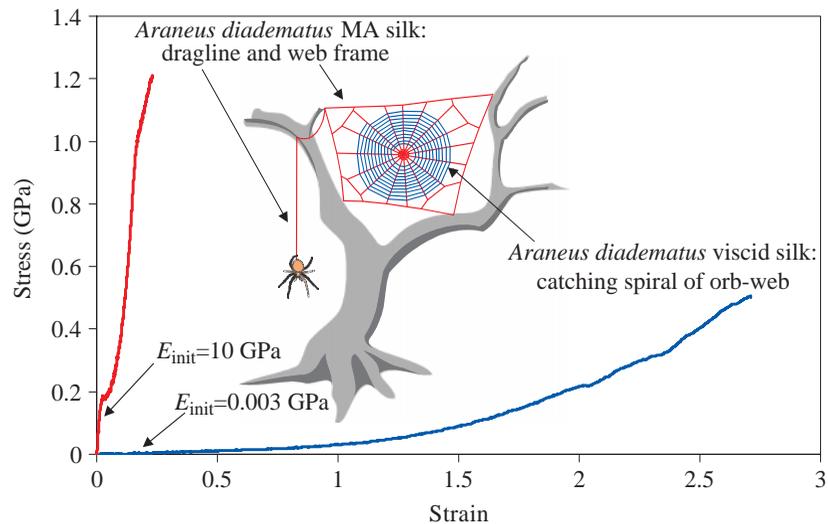
Fig. 1. Stress–strain curves for major ampullate (MA) gland (red line) silk and viscid silks (blue line) from the spider *Araneus diadematus*. E_{init}, initial stiffness.

achieve greater stiffness than this silk. The strength of MA silk, however, is clearly superior to that of all other biomaterials in this list, suggesting that strength, and to a lesser degree stiffness, may be important indicators of its mechanical performance. This list of biomaterials is incomplete, but it is fair to say that spider MA silk is amongst the stiffest and strongest polymeric biomaterials known. Note, however, that the stiffness of MA silk is well below that of Kevlar, carbon fibre and high-tensile steel, engineering materials that are commonly employed to transmit and support tensile forces. Note also that the strength of MA silk is somewhat less than that of these engineering materials. At first glance, we might interpret this information as indicating that MA silk is superior to other biomaterials, such as collagen, but not as 'good' as Kevlar and carbon fibres. However, this interpretation is based on the assumption that 'good' means stiff and strong.

Looking further along Table 1, we see that *Araneus* MA silk is quite extensible, failing at a maximal strain of approximately 0.27 (i.e. 27 % extension), whereas the engineering materials fail at strains of the order of 0.01–0.03. The large extensibility of MA silk, in spite of its somewhat inferior strength, makes MA silk tougher than the engineering materials. Indeed, with an energy to breakage (toughness) of 160 MJ m^{-3}, MA silk is 3–10 times tougher than its engineering counterparts. This suggests that energy absorption and toughness may be the crucial properties that will lead us to an understanding of the function of MA silk.

The viscid silk provides an interesting contrast in properties, and yet it also is a material with exceptional toughness. Its initial stiffness, at 0.003 GPa, is three orders of magnitude lower than that of MA silk and is comparable with that of a lightly crosslinked rubber. Indeed, viscid silk is best thought

Table 1. *Tensile mechanical properties of spider silks and other materials*

Material	Stiffness, E_{init} (GPa)	Strength, σ_{max} (GPa)	Extensibility, ε_{max}	Toughness (MJ m^{-3})	Hysteresis (%)
Araneus MA silk	10	1.1	0.27	160	65
Araneus viscid silk	0.003	0.5	2.7	150	65
Bombyx mori cocoon silk	7	0.6	0.18	70	
Tendon collagen	1.5	0.15	0.12	7.5	7
Bone	20	0.16	0.03	4	
Wool, 100 % RH	0.5	0.2	0.5	60	
Elastin	0.001	0.002	1.5	2	10
Resilin	0.002	0.003	1.9	4	6
Synthetic rubber	0.001	0.05	8.5	100	
Nylon fibre	5	0.95	0.18	80	
Kevlar 49 fibre	130	3.6	0.027	50	
Carbon fibre	300	4	0.013	25	
High-tensile steel	200	1.5	0.008	6	

The data for *Araneus* silks are from Denny (1976) and our laboratory. Other data have been taken from Wainwright et al. (1982), Gordon (1978, 1988) and Vincent (1982), without specific references because they are intended to indicate the relative magnitude rather than exact values.

MA silk, silk from the major ampullate gland; RH, relative humidity.

of as a rubber-like material. With a maximum strain of approximately 2.7, viscid silk is not exceptionally stretchy compared with other rubbery materials, but its strength, at approximately 0.5 GPa, makes viscid silk roughly 10 times stronger than any other natural or synthetic rubber. In this context, viscid silk is a truly remarkable material, and the combination of high strength and extensibility gives it a toughness virtually identical to that of MA silk fibres.

Mechanical function of MA and viscid silks

To understand the roles that extensibility and toughness play in the function of MA and viscid silks, we must consider the way that these fibres are used in the normal activities of spiders. As documented by Denny (1976), the MA silk fibres in an orb-web often experience loads at right angles to their long axis, and this imposes an interesting constraint on the properties of the fibre. For example, the weight ($m\mathbf{g}$, where m is mass and $\mathbf{g}$ is the acceleration due to gravity) of a spider hanging from a horizontal guy line (Fig. 2A) will cause a load (l) that deflects the web fibre downwards, stretching the fibre and causing a force (F_{silk}) to develop. $F_{silk}=l/2\sin\theta$, where θ is the deflection angle. For fibres with low extensibility, θ will be small, and F_{silk} can be much larger than the load l. Denny (1976) showed that the load is maximized with fibres having an extensibility ε_{max} of 0.42, and that the ε_{max} of 0.27 for MA silk allows the guy line to support a near-maximal load. For

comparison, a Kevlar fibre that had exactly the same breaking tension, but with $\varepsilon_{max}=0.027$, would support a load of less than 40 % of that supported by the MA silk. Fibre extensibility can compensate for strength when fibres are loaded normal to their long axis.

A similar situation holds in prey capture when a flying insect strikes a silk fibre in the web, again usually approximately at right angles to the fibre axis (Fig. 2B). The role of the web fibre is to absorb the kinetic energy of the insect's forward velocity, bringing the insect to a halt so that the spider can capture it. Clearly, the extreme toughness of both MA and viscid silks allows the spider to absorb a large amount of the prey's kinetic energy with a minimal volume of silk, but another important consideration is the manner in which this energy is absorbed. The energy could either be stored through elastic deformation or it could be dissipated as heat through friction. Load cycle experiments by Denny (1976) (Fig. 2C) indicate that the hysteresis for both MA and viscid silks is approximately 65 % (Table 1). That is, 65 % of the kinetic energy absorbed is transformed into heat and is not available to catapult the prey out of the web through elastic recoil.

The key properties of web silks that emerge from our analysis of web function involve a balance between strength and extensibility, giving enormous toughness, and a high level of internal molecular friction, giving high levels of hysteresis. Taken together, these properties are more consistent with a viscoelastic material than with the engineering materials listed in Table 1, and one of the key features of viscoelastic materials is that their properties vary strongly with the rate of deformation. In contrast, engineering materials are selected to have high stiffness and strength at the expense of extensibility, and they achieve this by having an extremely rigid molecular structure that virtually excludes the possibility of large-scale molecular motion.

Could the viscoelasticity of web silks be an important functional property? The answer is very probably yes, if strain-rate-dependent changes in properties enhance the functional capabilities of the web materials. Denny's (1976) analysis of the strain-rate-dependence of MA silk demonstrated that stiffness, strength, extensibility (extension to failure) and toughness (energy to failure) all increase as strain rate increases from $0.0005\,s^{-1}$ to $0.024\,s^{-1}$ (Table 2), suggesting that the performance of MA silk may indeed be enhanced by increasing strain rate. At the highest strain rate ($0.024\,s^{-1}$), a test to failure would take approximately 11 s. The events involved in prey capture or during the fall of a spider against its dragline will certainly occur over a much shorter time scale and therefore at a much higher strain rate. We recently developed an impact apparatus that loads MA silk fibres normal to the fibre axis with a falling object travelling at a velocity of approximately $1\,m\,s^{-1}$. Impact at this velocity causes failure after approximately 0.02 s, with strain rates of the order of $30\,s^{-1}$. Our experiments are currently in progress, but preliminary results indicate strong strain-rate-dependence, as shown in Fig. 3 and Table 2. The initial stiffness rises dramatically, as does the strength, and in exceptional tests the
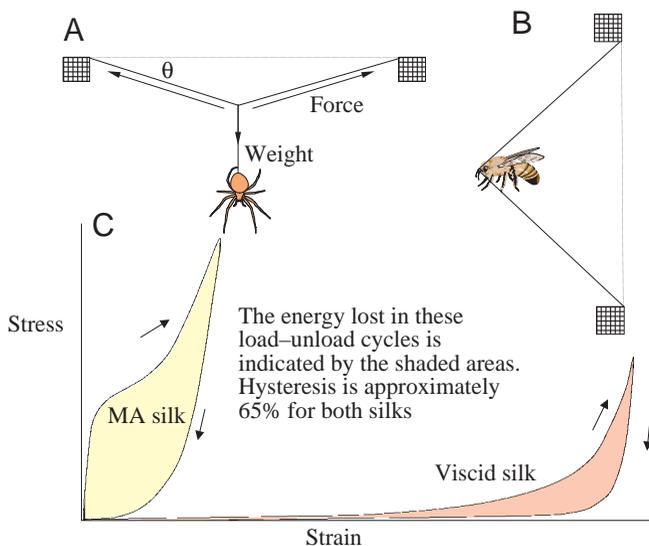
Fig. 2. Functional loading of *Araneus diadematus* major ampullate (MA) gland silk. (A) When a static load is applied at right angles to the fibre, fibre extension allows a large deflection angle θ, and the fibre is able to support a large load. (B) When a flying insect impacts a web element and is brought to a halt by the deflection of a silk fibre, the silk absorbs the kinetic energy ($E_K=0.5mV^2$, where E_K is kinetic energy, m is mass and V is velocity) of the insect. (C) The viscoelastic nature of this MA silk transforms much of this energy into heat through molecular friction. The energy dissipated is indicated by the area of the shaded loops in the stress–strain curves for load cycle experiments. Hysteresis is the ratio of the energy dissipated to the energy absorbed.

Table 2. *Strain-rate-dependent material properties of spider MA silks*

Properties	Araneus				Nephila clavipes	
	Strain rate					
	$0.0005\,s^{-1}$	$0.002\,s^{-1}$	$0.024\,s^{-1}$	$20–50\,s^{-1}$	$0.1\,s^{-1}$	$\approx 3000\,s^{-1}$
Initial stiffness, E_{init} (GPa)	9.8	8.9	20.5	25–40	22	20
Strength, σ_{max} (Gpa)	0.65	0.72	1.12	2.0–4.0	1.3	
Extension to failure, ε_{max} (%)	24	24	27	20–50	12	10
Energy to failure (toughness) (MJ m^{-3})	91	106	158	500–1000	80	

The first three columns of *Araneus* data are for *Araneus seriaticus*, taken from Denny (1976), and the strength data have been converted to engineering stress. The fourth column is for *A. diadematus*, from this study.

The *Nephila clavipes* data are from Cunnliff et al. (1994).

MA silk, silk from the major ampullate gland.

strength now virtually matches that of Kevlar and the toughness reaches the astronomical level of approximately 1000 MJ m^{-3}. Thus, to summarize, our analysis of the mechanical properties and mechanical function of MA and viscid silk fibres indicates that these materials have probably been selected through evolution to achieve a harmonious balance (Wainwright, 1988) of strength, extensibility and viscoelasticity, which together produce materials of incredible toughness.

One final set of properties remains to be considered. These are the responses of silk fibres to environmental variables such as temperature, moisture, etc. To date, little is known about the temperature-dependence of the mechanical properties of silks, although the strong strain-rate-dependence suggests that temperature changes will alter the mechanical properties. Water content, however, is known to have a major effect on MA silks (Work, 1977). When MA silk is immersed in water,

it shrinks by approximately 40–50 %, and its mechanical properties change markedly. The initial stiffness drops by three orders of magnitude, and the material becomes rubber-like in its behaviour (Gosline et al., 1984). Viscid silk also contracts when immersed in water, although the effect on its mechanical properties is less dramatic (Gosline et al., 1994, 1995). Work (1977) called this transition supercontraction, and to date no-one has discovered or described a function for supercontraction. Supercontraction will occur in air if the relative humidity reaches a level of approximately 90 % or more and, therefore, it is likely that the silk fibres in the webs of spiders may experience conditions for supercontraction in their normal use. The consequences of supercontraction in the orb-web are not known but, because the web is always tethered to rigid external structures and is laid down in tension (Denny, 1976), neither the MA silk nor the viscid silk will be able to shorten significantly. They will, however, develop a small

Fig. 3. Selected high-strain-rate impact tests of *Araneus diadematus* major ampullate (MA) gland silk that spans the range of behaviour observed. The low-strain-rate curve illustrates the magnitude of the increase in stiffness and strength. The inset diagram shows the experimental arrangement with the silk fibre supported between two force transducers, one that senses vertical force (F_v) and the other that senses horizontal force (F_h). Fibre force (F_{silk}) and fibre strain are calculated trigonometrically. L_0, unstretched length.
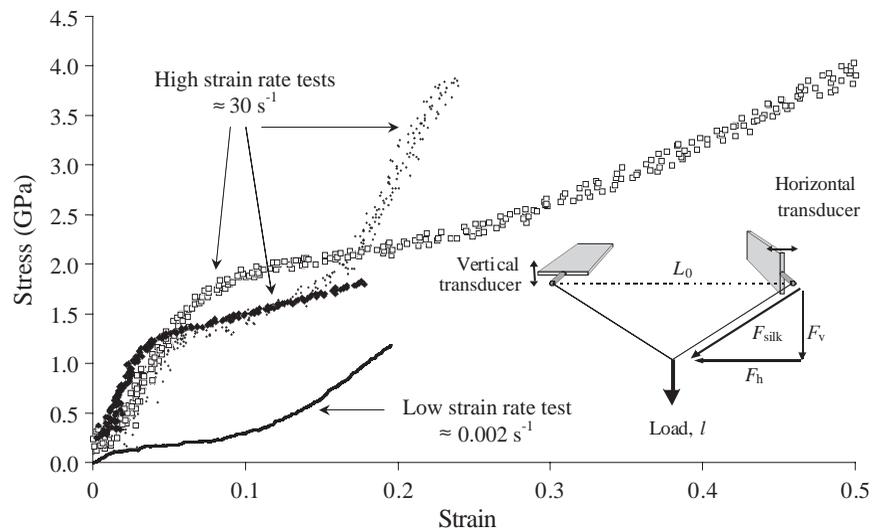
additional tension that may serve to keep the web taut, and the increased water content may reduce the level of hysteresis and alter the strain-rate-dependence described above.

Much remains to be learned, but it is possible that supercontraction is simply an unavoidable consequence of the molecular structure required to create the balance of mechanical properties described above. We know that the design of these silks requires a structure that allows considerable movement at the molecular level to provide high levels of toughness and energy dissipation. Perhaps this level of molecular movement could only be achieved with a protein sequence that incorporates a large fraction of polar amino acids, thus imparting the hydration-sensitivity that creates supercontraction. Whatever the role or origin of supercontraction, it is important to note that this tendency of spider MA silk to absorb water, shrink and become rubbery may strongly limit the utility of this design for application to man-made materials.

The molecular architecture of spider silks

X-ray diffraction studies have shown that virtually all silks contain protein crystals, and the majority of these silks contain β-pleated sheet crystals that form from tandemly repeated amino acid sequences rich in small amino acid residues. For example, textile silk produced by the silk moth *Bombyx mori* contains multiple repeats of the hexapeptide motif GAGAGS (where G is glycine, A is alanine and S is serine). Further, it is well established that the alternation of glycine with either alanine or serine causes this sequence spontaneously to form β-pleated sheet crystals (see Wainwright et al., 1982; Kaplan et al., 1994). In *B. mori* silk, these protein crystals occupy 40–50 % of the total volume of the silk fibre (Iizuka, 1965), with the remainder being occupied by protein chains having a much less ordered, possibly amorphous, structure. Recent developments in the study of spider silks are beginning to reveal the molecular origins of their material properties.

Network models for supercontracted MA silk

One major problem in defining the molecular structure of silk fibres has been a lack of information on the structure and volume fraction of the 'amorphous domains' that exist between the crystals in silk fibres. Analysis of the mechanical properties of supercontracted MA silk reveals that the amorphous domains are a dominant feature of *Araneus diadematus* MA silk. Because hydrated MA silk exists in a rubber-like state (Gosline et al., 1984), it is possible to use the theory of rubber elasticity (Treloar, 1975) to develop a model for the protein network in MA silk. In addition, because the crystals are not altered during supercontraction, it is possible to apply this model to the organization of the native silk fibres. The modelling process is based on the tendency of rubber networks to become increasingly stiff when the network chains approach their full extension. Details of this analysis are described elsewhere (Gosline et al., 1994, 1995); only the essence of the molecular models is described here.

The *A. diadematus* MA silk network models are illustrated in Fig. 4, and they have the following features. First, MA silk contains a crystal-crosslinked and crystal-reinforced polymer network. That is, the crystals form the intermolecular connections between the fibroin molecules, and the crystals are large enough and abundant enough to act as reinforcing filler particles to stiffen and strengthen the network. The amorphous chains, which interconnect the crystals, are estimated to be 16–20 amino acid residues long, and the water absorbed during supercontraction is associated primarily with these amorphous chains. The rubber-like elasticity of the hydrated network arises from the large-scale extension of these coiled amorphous chains. The crystals are estimated to have a length/width ratio of approximately 5, and they occupy approximately 10–12 % of the volume of the hydrated MA silk (Fig. 4A).

The model for the native state of the MA silk fibre is created by applying an 80 % stretch to regain the native length, and by shrinking the model laterally to account for the loss of approximately 50 % of the volume when the water evaporates (Fig. 4B). This produces a crystal volume fraction of 20–25 %. The amorphous chains are extended, and the polymer crystals are rotated during the stretching and shrinking to produce a strongly preferred molecular orientation parallel to the fibre axis. The physical state of the extended, amorphous chains remains to be determined, but one possibility is that they form a rigid, extended polymeric glass phase, creating a highly oriented, fibre-reinforced polymer network. It is likely that this model can explain both the mechanical properties described above and the fibroin sequence designs described below.

Molecular genetics of the spider fibroin gene family

Until recently, we knew little about the amino acid sequence motifs in spider fibroins, although we knew that each of the seven glands produced proteins with unique amino acid compositions (Andersen, 1970). The compositions of most spider silks are similar to that of the textile silk produced by the silk moth *B. mori*, but with some significant differences in the abundance of the larger and more polar amino acid residues. *B. mori* fibroin is known to contain multiple repeats of a hexapeptide and, as shown in Fig. 5, the hexapeptide GAGAGS occurs in blocks of 8–10 repeats, separated by another repeating motif that is somewhat more variable. These two large sequence blocks repeat four or five times between a small, approximately 30 residue, section of non-repetitive sequence called the 'amorphous domain' (Mita et al., 1994). Thus, *B. mori* fibroin contains a preponderance of long crystal-forming blocks, which establishes a strong potential for crystal formation, and this probably accounts for the high crystal content of *B. mori* silk.

Recently, sequence data for two MA silk fibroins from the araneid spider *Nephila clavipes* (Xu and Lewis, 1990; Hinman and Lewis, 1992) have revealed that the sequence designs of spider fibroins are fundamentally different from those of *B. mori* fibroin. Sequences from two genes expressed in the *N. clavipes* MA gland (Nc-MA-1 and Nc-MA-2) reveal repeating sequence motifs approximately 34 and 45 amino acid residues

A

B

Amorphous
network chains:
16–20 amino acid
residues long

Water: 50% of
total volume

β-sheet crystals:
crosslink and reinforce
the polymer network

Supercontracted MA silk:
crystal volume fraction is 10–12%

Native MA silk:
crystal volume fraction
is 20–25%

Fig. 4. Models for the molecular architecture of *Araneus diadematus* major ampullate (MA) gland silk. (A) When immersed in water, MA silk supercontracts, i.e. it swells, shrinks and becomes rubbery. Analyses of the mechanical and optical properties of supercontracted silk provide information on the nature of the amorphous chains and the size and orientation of the β-sheet crystals in the silk polymer network. (B) Model of the native MA silk fibre obtained by extending and 'drying' the model derived for the supercontracted state.

long, respectively (Fig. 5). Within each repeat motif, there is a short poly-alanine block, 8–10 residues in length (highlighted yellow), that we now know forms a very short crystal-forming domain. The remainder of the repeat motif contains a glycine-rich domain that is probably very different in its crystal-forming potential and may direct the formation of amorphous domains in the MA silk polymer network. Thus, the repeat motifs contain approximately one-quarter of their sequence in the form of crystal-forming elements, and these crystal-forming elements are very short.

More recently, Guerette et al. (1996) reported repeating sequence motifs for fibroins from the spider *A. diadematus* (Fig. 5), showing that the pattern of small crystal-forming blocks alternating with larger 'amorphous' blocks is a feature of spider silk fibroins produced in at least three silk glands, the MA gland, the minor ampullate (MI) gland and the cylindrical (CY) gland. Interestingly, different silk glands express fibroins with different proportions of crystal-forming and amorphous sequence elements, imparting different tendencies for the formation of crystals in their silk fibres. For example, the two fibroins found in *A. diadematus* MA silk (Ad-MA-1 and Ad-MA-2) have similar proportions to those produced by *N. clavipes*, with crystal-forming elements occupying approximately one-quarter of the repeat block. The *A. diadematus* MI fibroin (Ad-MI-1) has a much larger fraction of crystal-forming blocks (68 %) and very short amorphous blocks (32 %), a pattern that has been documented recently for *N. clavipes* MI silk (Nc-MI-1 and Nc-MI-2; Colgin and Lewis, 1998). The high crystal-forming content of MI silk fibroins probably accounts for the fact that spider MI silks are more birefringent than MA silks and that MI silks do not

supercontract when they are immersed in water (Work, 1977), properties that reflect a high crystal content.

Major ampullate gland (MA) fibroins

Nc-MA-1: AGAAAAAAAGGAGQGGYGGLGSQGAGRGGLGGQG

Nc-MA-2: SAAAAAAAAAGPGGYGPGQQPGGYGPGQQQPGGYGPGQQQPSGPG

Ad-MA-1: ASAAAAAAAGGYGPGSGQQGPGQQGPGGQGPYGP

Ad-MA-2: ASAAAAAAAAASGPGGYGPGSQGPSGPGGYGPGGPG

Minor ampullate gland (MI) fibroins

Nc-MI-1: AGAGAGAAAGAGAGGYGGQGGYGAGAGAGAAAAAGAGGAGGYGRG

Nc-MI-2: AVAGSGSAAGAGARACSGGYGGQGGYGAGAGAGAAAGAGAGSAGGYGRG

Ad-MI-1: GAGSGAGAGAAAAAGAGGYGQGY

Cylindrical gland (CY) fibroin

Ad-CY-1: AAAAAAAAGGQGGQGGYGGLGSQGGAGQGGYGAAGLGGQGG

Flagelliform gland (FL) fibroin

Nc-FL-1: $(GPGGX)_{N \approx 50}$ - $(GGX)_{N \approx 9}$ - $(Spacer, 28 \text{ residues long})$

***Bombyx mori* cocoon silk fibroin**

$\{(GAGAGS)_{N=8-10}$ - $[(GA)_{N=1-3} - GY]_{N=4-7}\}_{N=4-5}$ - $(Spacer)$

Fig. 5. Amino acid sequence motifs for spider silk fibroins. Crystal-forming motifs are highlighted in yellow; proline residues are highlighted in purple. The Nc-MA-1 data are taken from Xu and Lewis (1990), the Nc-MA-2 data are from Hinman and Lewis (1992), the Nc-MI-1 and Nc-MI-2 data are from Colgin and Lewis (1998), and the Nc-FL-1 data are from Hayashi and Lewis (1998). All Ad-MA, Ad-MI and Ad-Cy data are taken from Guerette et al. (1996). The *Bombyx mori* heavy-chain fibroin data are taken from Mita et al. (1994). G, glycine; A, alanine; S, serine; P, proline; Q, glutamine; Y, tyrosine; L, leucine; V, valine; R, arginine. *X* can be alanine, serine, valine or tyrosine.

The repeat motifs for *A. diadematus* MA fibroins (Ad-MA-1 and Ad-MA-2) provide an opportunity to evaluate the network model for supercontracted MA silk shown in Fig. 4. The amorphous chains between crystals were predicted to be 16–20 amino acid residues long, and the crystals were predicted to occupy 20–25 % of the total volume in the native fibre. The poly-alanine blocks in the Ad-MA repeats account for 25–30 % of the total, and the glycine-rich amorphous blocks are 24–25 residues in length, a reasonable match between the inferred polymer network and the fibroin sequences.

Recently, Hayashi and Lewis (1998) obtained sequence information for a fibroin from the flagelliform (FL) gland (viscid silk core fibre: Nc-FL-1, Fig. 5). This fibroin is almost entirely constructed from glycine-rich sequence motifs characteristic of the amorphous blocks in MA fibroins. That is, there are numerous (40–65) repeats of the pentapeptide GPGG*X* (where P is proline and *X* can be alanine, serine, valine or tyrosine), and this huge amorphous domain is followed by a second glycine-rich motif, GG*X*, that is repeated 6–12 times. There are no obvious crystal-forming domains that look like any found in spider MI, MA or CY silks, and we are left to consider the source of the crosslinking that must certainly exist in viscid silk to explain its exceptional strength. Network models developed for *A. diadematus* viscid silk (Gosline et al., 1994, 1995) suggest that the network chains probably contain 50–75 amino acid residues between crosslinks, but this number is considerably smaller than the size of the pentapeptide repeat blocks observed in Nc-FL-1 (approximately 240–350 residues). Perhaps the sequence design is different in *A. diadematus* FL fibroins, or perhaps we have much learn about the organization of FL silks.

We can now consider the correlation between sequence design and mechanical properties. The network structure of *A. diadematus* MA silk contains a low volume fraction of very small crystals separated by rather long amorphous chains, and perhaps this structure is responsible for the fact that *A. diadematus* MA silks are respectably strong but are incredibly tough and viscoelastic. If the amorphous network chains behave as an extended polymeric glass, then deformation of these chains could account for the high extensibility of MA silk and could also explain its high level of hysteresis. Note also that the glycine-rich motifs in both Ad-MA-1 and Ad-MA-2 contain numerous polar glutamine residues (glutamine, Q), and these will explain the tendency of MA silk to absorb water and supercontract. *B. mori* silk, with its extremely long crystal sequences and high crystallinity, does not match spider MA silk for stiffness, strength or extensibility (Table 1), and the highly crystalline MI silk is no stronger than MA silk (Work, 1977). Clearly, crystallinity is not the only important feature of network design in spider MA silks. Amorphous chains that allow deformation and viscoelastic energy dissipation are equally important features of MA silk designs.

Physical characterization of the MA silk network

The remarkable success of the biotechnology community in the synthesis of genetically engineered silk fibres based on the MA fibroin sequences from *N. clavipes* (Lipkin, 1996) has generated an enormous interest in the structure of this material. As a consequence, we know more about *N. clavipes* MA silk than any other spider silk. X-ray diffraction indicates that the β-sheet crystals have an inter-sheet spacing of 0.53 nm, a spacing characteristic of β-sheet crystals formed from poly-alanine (Becker et al., 1994). Detailed analyses of X-ray patterns indicate that the crystal dimensions are approximately 2 nm×5 nm×7 nm, a scale consistent with β-sheets formed from the short poly-alanine blocks seen in the fibroin sequences and having a length/width ratio similar to that predicted in the network models. The crystals are strongly aligned with the fibre axis and occupy 10–15 % of the total volume (Grubb and Jelinsky, 1997; Yang et al., 1997). These conclusions are confirmed by nuclear magnetic resonance (NMR) studies (Simmons et al., 1996; Kummerlen et al., 1996); however, it is not clear whether the fibre contains a simple two-component (crystal + amorphous) structure. Simmons et al. (1996) observed two populations of alanine residues in their NMR spectra, only one of which could be considered to be the highly ordered and oriented crystals depicted in Fig. 4. Apparently, only approximately 40 % of the alanine residues are present in the oriented β-sheet crystals, with the remaining 60 % found in weakly oriented and unaggregated β-sheets. This would suggest that the total crystal content is higher than the 10–15 % noted above, and it may explain why the network models based on mechanical tests (Fig. 4) predict a crystal content of 20–25 %. It is probably safe to extend these general conclusions to the MA silks of *A. diadematus* since the Ad-MA fibroins contain poly-alanine blocks of virtually identical dimensions to those of *N. clavipes*, but the details may vary somewhat.

The idea that the sequence data could predict the structural organization of the 'amorphous' glycine-rich domains is, however, an oversimplification. Kummerlin et al. (1996) employed two-dimensional NMR to study *N. clavipes* MA silk and discovered strong evidence for an ordered microstructure in the glycine-rich domains. They concluded that the simplest model to fit their experimental data is a 3_1-helical structure, and they speculate that these 3_1-helices aggregate to reinforce the highly oriented polymer network present in MA silk. An alternative hypothesis has been put forward by Thiel et al. (1996) on the basis of electron diffraction and an analysis of the minor peaks in the X-ray diffraction pattern of *N. clavipes* MA silk. They suggest that, when stretched, the glycine-rich sequences are able to form large-scale β-sheet crystal structures that are less perfectly ordered than the poly-alanine crystals described above. They consider *N. clavipes* MA silk to be a hierarchical structure in which the poly-alanine crystals are surrounded by a 'non-periodic crystal lattice' formed in the glycine-rich sequences. A key feature of these proposals is that the glycine-rich sequences should not contain proline. That is, the structural proposals for the 'amorphous' regions of *N. clavipes* MA silk apply to only one of the MA fibroins, namely Nc-MA-1, as this is the only fibroin without proline in its

glycine-rich domains. The other three MA fibroins (Nc-MA-2, Ac-MA-1 and Ad-MA-2) all contain 15–17 % proline (Fig. 5; highlighted in purple) in their repeat motifs.

N. clavipes MA silk has a very low total proline content (approximately 3 %), whereas *A. diadematus* MA silk has a proline content (16 %) that just matches the content of its two fibroins. This difference in proline content has major consequences for the two MA silks. *N. clavipes* MA silk is apparently made primarily of Nc-MA-1, the proline-free fibroin, and the proposals for the presence of ordered structures in the glycine-rich domains are reasonable. *A. diadematus* MA silk contains fibroins with a high proline content, and this should prevent the formation of similar ordered structures in the *A. diadematus* silk network. Thus, the simple amorphous + crystal network model for *A. diadematus* MA silk in Fig. 4 is probably correct, but it probably does not apply to *N. clavipes* MA silk.

If the high extensibility, viscoelasticity and energy dissipation of *A. diadematus* MA silk are due to the truly amorphous organization of the network chains between crosslinking crystals, then *N. clavipes* MA silk may have quite different mechanical properties. This indeed appears to be the case. Mechanical testing of *N. clavipes* MA silk (Cunnliff et al., 1994) indicates that it has a greater initial stiffness ($E_{init}=22\,\mathrm{GPa}$) and a lower extensibility ($\varepsilon_{max}=0.12$) but a similar strength to *A. diadematus* MA silk, yielding a toughness approximately half that of *A. diadematus* MA silk (see Table 2). These properties are consistent with a more structured or crystalline network in *N. clavipes* MA silk. These workers also report a value for stiffness and extensibility of *N. clavipes* MA silk in a ballistic test at a strain rate of approximately $3000\,\mathrm{s}^{-1}$ (Table 2), and it appears that *N. clavipes* silk shows little strain-rate-dependence for stiffness and a slight decline in extensibility. This could be another consequence of a more crystalline network structure, and it suggests that *N. clavipes* MA silk is less effective at dissipating impact energies.

An important conclusion to draw from this comparison of *A. diadematus* and *N. clavipes* MA silks is that we should be careful in developing structure–function relationships from the experimental data available at this time. Our knowledge of function of is based on experiments with *A. diadematus* MA silk, and our knowledge of ordered structure in the glycine-rich domains is based on experiments with *N. clavipes* silk. We should wait until we have a more balanced understanding of the function of *N. clavipes* silk and the structure of *A. diadematus* silks.

Conclusion

Our knowledge of spider silk molecular biology and silk network structure is growing rapidly and it may, in time, provide a rational basis for the design of structural materials through genetic engineering. There are two paths to achieve this goal. Through a purely synthetic approach, a variety of sequence motifs could be designed, expressed, spun into fibres and then tested for desirable mechanical properties.

Alternatively, we could build upon the variation created through millions of years of evolution to develop an understanding of structural designs that already exist in nature and have been tested in the day-to-day function of spiders. The comparison between *N. clavipes* and *A. diadematus* MA silks outlined here shows that this second approach will work if we have sufficient information about the true function of the silks of spiders. Spider fibroin genes belong to a single gene family (Guerette et al., 1996; Hayashi and Lewis, 1998), so it should be easy to obtain fibroin sequence information from related spider species. If our knowledge of functional biomechanics and of silk network structure can keep pace, then the diversity that exists in living spiders should help us to develop a full understanding of protein-based structural materials.

References

Andersen, S. O. (1970), Amino acid composition of spider silks. *Comp. Biochem. Physiol.* **35**, 705–714.

Becker, M. A., Mahoney, D. V., Lenhert, P., Eby, R., Kaplan, D. and Adams, W. (1994). X-ray modulus of silk fibers from *Nephila clavipes* and *Bombyx mori*. In *Silk Polymers* (ed. D. Kaplan, W. W. Adams, B. Farmen and C. Viney), pp. 185–195. Washington, DC: American Chemical Society.

Colgin, M. A. and Lewis, R. (1998). Spider minor ampullate silk proteins contain new repetitive sequences and highly conserved non-silk-like 'spacer regions'. *Protein Sci.* **7**, 667–672.

Cunnliff, P. M., Fossey, S. A., Auerbach, A., Song, J. W., Kaplan, D., Adams, W., Eby, D. and Vezie, D. (1994). Mechanical and thermal properties of dragline silk from *Nephila clavipes*. *Polymers Adv. Technol.* **5**, 401–410.

Denny, M. (1976). The physical properties of spider's silk and their role in the design of orb-webs. *J. Exp. Biol.* **65**, 483–506.

Gordon, J. E. (1978). *Structures*. Middlesex, UK: Penguin Books. 395pp.

Gordon, J. E. (1988). *The Science of Structures and Materials*. New York: W. H. Freeman. 217pp.

Gosline, J. M., DeMont, M. E. and Denny, M. W. (1986). The structure and properties of spider silk. *Endeavour* **10**, 37–43.

Gosline, J. M., Denny, M. and DeMont, M. E. (1984). Spider silk as rubber. *Nature* **309**, 551–552.

Gosline, J. M., Nichols, C., Guerette, P., Cheng, A. and Katz, S. (1995). The macromolecular design of spider's silks. In *Biomimetics: Design and Processing of Materials* (ed. M. Sarikaya and I. Aksay), pp. 237–262. Woodbury, New York: American Institute of Physics.

Gosline, J. M., Pollak, C. C., Guerette, P., Cheng, A., DeMont, M. E. and Denny, M. W. (1994). Elastomeric network models for the frame and viscid silks from the orb web of the spider *Araneus diadematus*. In *Silk Polymers: Materials Science and Biotechnology* (ed. D. Kaplan, W. Adams and C. Viney), pp. 328–341. Washington, DC: American Chemical Society.

Grubb, D. T. and Jelinsky, L. W. (1997). Fiber morphology of spider silk – the effect of tensile deformation. *Macromolecules* **30**, 2860–2867.

Guerette, P., Ginzinger, D., Weber, B. and Gosline, J. M. (1996).

The spider silk fibroin gene family: gland specific expression controls silk properties. *Science* **272**, 112–115.

Hayashi, C. Y. and Lewis, R. (1998). Evidence from flagelliform silk cDNA for the structural basis of elasticity and modular nature of spider silks. *J. Mol. Biol.* **275**, 773–784.

Hinman, M. and Lewis, R. (1992). Isolation of a clone encoding a second dragline silk fibroin. *J. Biol. Chem.* **267**, 19320–19324.

Iizuka, E. (1965). Degree of crystallinity and modulus relationships of silk threads from *Bombyx mori. Biorheology* **3**, 1–8.

Kaplan, D., Adams, W. W., Farmen, B. and Viney, C. (1994). *Silk Polymers*. Washington, DC: American Chemical Society. 370pp.

Kummerlin, J., van Beek, J., Vollrath, F. and Meier, B. H. (1996). Local structure in spider dragline silk investigated by 2-dimensional spin-diffusion NMR. *Macromolecules* **29**, 2920–2928.

Lipkin, R. (1996). Artificial spider silk. *Sci. News* **149**, 152–153.

Mita, K., Ichimura, S. and James, T. (1994). Highly repetitive structure and its organization of the silk fibroin gene. *J. Mol. Evol.* **38**, 583–592.

Simmons, A. H., Michal, C. A. and Jelinski, L. W. (1996). Molecular orientation and two-component nature of the crystalline fraction of spider dragline silk. *Science* **271**, 84–87.

Thiel, B. L., Guess, K. B. and Viney, C. (1996). Non-periodic lattice crystals in the hierarchical microstructure of spider MA silk. *Biopolymers* **41**, 703–719.

Treloar, L. R. G. (1975). *Physics of Rubber Elasticity*. Oxford: Oxford University Press. 310pp.

Vincent, J. (1982). *Structural Biomaterials*. Princeton, NJ: Princeton University Press. 204pp.

Vollrath, F. (1992). Spider webs and silks. *Scient. Am.* **266**, 70–76.

Wainwright, S. A. (1988). *The Axis and Circumference*. Cambridge, MA:Harvard University Press. 132pp.

Wainwright, S. A., Biggs, W. D., Currey, J. D. and Gosline, J. M. (1982). *Mechanical Design in Organisms*. Princeton, NJ: Princeton University Press. 423pp.

Work, R. W. (1977). Dimensions, birefringence and force–elongation behaviour of major and minor ampullate silk fibres from orb-web spinning spiders. *Text. Res. J.* **47**, 650–662.

Xu, M. and Lewis, R. (1990). Structure of a protein superfiber: spider dragline silk. *Proc. Natl. Acad. Sci. USA* **87**, 7100–7124.

Yang, Z., Grubb, D. T. and Jelinsky, L. W. (1997). Small angle X-ray scattering of spider dragline silk. *Macromolecules* **30**, 8254–8261.